Instability Detector of a Fragile Neural Network: Application to Seizure Detection in Epilepsy

Daniel Ehrens, Duluxan Sritharan and Sridevi V. Sarma *Member, IEEE*

***Abstract*— It has recently been proposed that the epileptic cortex is *fragile* in the sense that seizures manifest through small perturbations in the synaptic connections that render the entire cortical network unstable. Therefore, one method for detecting seizures is to detect when the neuronal network has gone unstable. This is important for implementing a closed-loop therapy to suppress seizures. In this paper, we consider a widely used nonlinear stochastic model of a neuronal network, and assume that spiking dynamics during non-seizure periods correspond to certain synaptic connections that render its fixed point stable. We then apply a minimum energy perturbation theory we recently developed for networks to determine the changes in the most *fragile* node's synaptic connections that make the same fixed point unstable (our model during seizure). Then a detector is designed as follows. First a 2-state HMM is constructed (stable=state 1 and unstable=state 2) with fixed state transition probabilities, where the output observation is the firing rate of the most fragile node in the network. The output density functions are assumed to be Gaussian with parameters computed using maximum likelihood estimation on data generated from the nonlinear network model in each state. Then, to detect a transition from stable to unstable, spiking activity is simulated in all nodes from the nonlinear model. The detector first measures the firing rate of the fragile node, and computes the derivative of the cumulative likelihood ratio of the observed firing rate from the HMM's output distributions. When the derivative exceeds a certain threshold, a transition to the unstable state is detected. Various thresholds were tested when firing rate was computed by averaging over a different number of windows of different lengths. High performance was achieved and a tradeoff was found between the accuracy of the detector and the detection delay.**

I. INTRODUCTION

Epilepsy is a neurological condition that affects approximately 70 million worldwide [1]. Approximately 20-30% of the population that has epilepsy suffers from intractable epilepsy where seizures cannot be controlled through medications. These patients must consider alternative and more invasive treatments such as resective surgery, deep brain stimulation (e.g., implanted responsive neurostimulators; RNS, NeuroPace, Mountain View, California) and vagal nerve stimulation [2]. Closed-loop stimulation systems for epilepsy rely mainly on early detection of the seizure onset in order to be able to disrupt the seizure before clinical manifestations occur [3]. To reliably detect seizure onsets, it is necessary to understand the electrophysiological dynamics in the cortical epileptic network.

Seizures are characterized by abnormal electrical activity in the brain, represented by synchronization of large neuronal populations [4]. However, single unit recordings show that during seizures there exists heterogeneity in neuronal firing patterns, where firing rate either increases, decreases or vanishes altogether [5]. It is clear that epilepsy is a network driven phenomenon in which ultimately the structural connectivity between neurons is altered [6], [7], [8], [9].

We recently constructed a neuronal network model of the epileptic cortex that qualitatively captured the heterogeneity in neurons observed in patients [10]. In [10], it is posited that the epileptic cortex is on the brink of instability such that small perturbations in the synaptic connections render the network unstable temporarily. This study envisions epilepsy as a chronic transitioning phenomenon between a stable state (non-seizure) and an unstable state (seizure). It is assumed that the cause of epilepsy is a specific structural change in the network, which happens to the most *fragile* node or neuron in the network. In [10], nodal *fragility* is defined as the minimum perturbation in functional connectivity that renders the network unstable, and the corresponding structural perturbation (i.e. changes in synaptic weights of the most fragile node) is computed. The model is a probabilistic nonlinear neuronal network model that operates at a stable fixed point during non-seizure mode. That is, if a small stimulus is applied to the network, after a transient response, it will return to the fixed point. When destabilized through synaptic weight perturbations of the most fragile node, the other nodes become either more or less active and the fragile node is silenced in response to a small stimulus.

The goal of this study is to build a detector that takes in spike train measurements from the probabilistic nonlinear neuronal network model and detects when the network goes unstable. To do so, we construct a two-state Hidden Markov Model (HMM) with an unstable state and a stable state. The output of the HMM is the firing rate of the most fragile node, which is generated by the network model, and is characterized by a Gaussian distribution in each state. When in the stable/unstable state, the network model is simulated in its stable/unstable mode to generate spike trains that are then averaged over windows to generate firing rates. The detector then computes the derivative of the cumulative likelihood ratio of the fragile node's firing rate from the HMM's output distributions, and when this measure is above a certain threshold, instability is detected.

Different thresholds and different scenarios were considered for computing the firing rate of the fragile node, until we found a set of high performing (i.e., minimal number of false positives and small delays between the seizure onset and its detection [11]) detectors. We found a clear tradeoff between

D. Ehrens, D. Sritharan, and S. V. Sarma are with the Department of Biomedical Engineering, Johns Hopkins University, Baltimore, MD 21218 USA (corresponding author: D. Ehrens; e-mail: dehrens@jhu.edu).

detection accuracy and detection delay. This work sets the stage for the design of a feedback control design that first detects instability and then applies an input (e.g. electrical stimulation) to the most fragile node in the network to return it to its stable fixed point.

II. METHODS

A. Neuronal Network Model

We considered a probabilistic network model as the one proposed in [12]. The model consists of a set of interconnected neurons (nodes), where each connection has a weighted edge that represents the synaptic strength between the two nodes. The internal activity of each node depends on its synaptic inputs and its current state. Let node *i* be a neuron that at some time *t* is either active $(x_i(t) = 1)$ or quiescent $(x_i(t) = 0)$. The transition between active and inactive states evolves as a Markov process with rate constants for a small time interval *dt*. The state probability is given by:

$$Pr\left\{(x_i(t+dt) = 0; x_i(t) = 1)\right\} = \alpha dt \quad (1)$$

$$Pr\left\{(x_i(t+dt) = 1; x_i(t) = 0)\right\} = f(s_i(t))dt \quad (2)$$

An active node represents the duration of a neuron's action potential including its refractory period. A node's activation propensity depends on its total synaptic input, represented by $s_i(t)$ defined below. The inactivation propensity is fixed, therefore a neuron on average is active for a period of α^{-1}. $f(\bullet)$ is a non-linear response function that represents the firing rate of a node when quiescent. For simulation purposes, a clamped hyperbolic tangent was used as in [10]. From (1) and (2), the probability of a neuron *i* being active at any time *t*, evolves according to the following nonlinear rate equation:

$$\dot{r}_i(t) = -\alpha r_i(t) + f(s_i(t))[1 - r_i(t)] \quad (3)$$

The network of *N* nodes is parameterized by the structural connectivity matrix, $\mathbf{W} = [w_{ij}]$. Each element in $\mathbf{W}$ describes the effect of node *j* on node *i*. Positive values represent excitation, negative values represent inhibition and a zero value means there is no connection between nodes *j* and *i*. The input to node *i*, s_i, depends on the state of the nodes that are connected to node *i*, the weight in its connections and an external input, h_i. If node *j* is active the synaptic input on node *i* is increased. Synaptic input is given by:

$$s_i(t) = \sum_{j=1}^{N} w_{ij} x_j(t) + h_i \quad (4)$$

A stable fixed point exists in this model where $\hat{r} \in \Re^N$ is a steady state probability that satisfies $g(\hat{r}; \mathbf{W}) = 0$ and represents the baseline behavior of the network. It is shown in [10] that $\hat{r}$ can be computed through a gradient descent algorithm that iterates candidate solutions to minimize a cost function.

Note that (3) estimates the functional activity of the network given some network structure, $\mathbf{W}$. By linearizing equation (3) around the fixed point, we obtain the functional connectivity matrix, $\mathbf{A}$. Then $\mathbf{A}$ has eigenvalues $\lambda_{1...N} \in \Im$ where $\Re\{\lambda_1\} \geq ... \geq \Re\{\lambda_N\}$. The functional connectivity matrix captures how the probability of any node being active affects the probability of node *i* being active. Since $\hat{r}$ is a stable fixed point then, $\Re\{\lambda_i(\mathbf{A})\} < 0$. In [10] the minimum energy functional perturbation needed to produce instability was determined and then the structural changes that would produce this functional perturbation were derived.

The minimum energy perturbation is done by applying a row perturbation Δ to $\mathbf{A}$. This represents a change in the inbound effect of the network on that node. The minimum perturbation takes $\Re\{\lambda_1(\mathbf{A} + \Delta)\} = 0$ where the system would be on the brink of instability. In [10], it is shown how Δ is computed using least squares.

To build the model of a neuronal epileptic network we used the connectivity matrices that were derived in [10]. In this study, we use one functionally stable structural matrix $(\mathbf{W}_s)$ and two functionally unstable structural matrices $(\mathbf{W}_{u0}, \mathbf{W}_{u200})$. Where, $\Re\{\lambda_1(\mathbf{W}_{u0})\} = 0$ Hz and $\Re\{\lambda_1(\mathbf{W}_{u200}\} = 200$ Hz. An inter-ictal stable state is simulated by using $\mathbf{W}_s$ in (3), and an ictal unstable state is simulated by using either $\mathbf{W}_{u0}$ or $\mathbf{W}_{u200}$

The network simulated here has 6 nodes, each a single neuron, and 14 connections. The model simulation follows the Gillespie stochastic algorithm [13].

The decay rate, α, is set to 100 Hz, which caps the neuronal firing rates at that value. Both $\mathbf{W}_{u0}$ and $\mathbf{W}_{u200}$ have a row perturbation at a DC frequency on node 4, an inhibitory neuron. Therefore when the unstable neuronal network is simulated the firing rate of this neuron decreases, thus inhibiting less, which increases firing activity in the network. All simulations were done using MATLAB.

B. HMM Representation of Epileptic Network

A two state HMM is constructed to represent an epileptic neuronal network. Fig. 1 shows a schematic of the HMM.

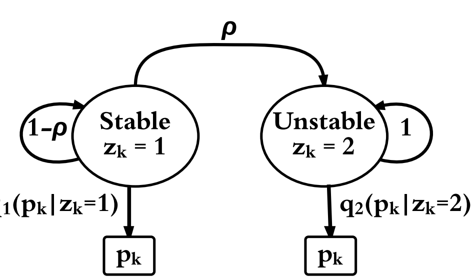

Fig. 1. HMM schematic with two states $(z_k = 1)$ and $(z_k = 2)$ and observable output p_k. $q_z(p_k)$ is the probability function of p_k in state $z \in \{1, 2\}$ and ρ is the probability of transition from state 1 to state 2.

The output observation is p_k, which is the firing rate of the most fragile node in the original nonlinear network described above, and it is obtained at discrete time steps

$k = 0, 1, 2, \ldots$ The network is in one of two states at each stage k; an inter-ictal stable state ($z_k = 1$) and an ictal unstable state ($z_k = 2$). We assume that the network initial state is always stable, that is, $z_0 = 1$ and it transitions to the unstable state with a fixed probability $\rho = 0.01$. Since we are only interested in detecting this transition, the HMM does not transition back to a stable state. The output density functions q_1 and q_2 are assumed to be Gaussian, and the parameters for these functions were computed using a maximum likelihood estimation from a 100 sec simulation of each state from the original nonlinear model.

C. Instability Detector

The input to the detector is p_k, which is obtained every time step from the spike train of the most fragile node. This is computed by retrospectively counting the number of spikes in an immediate fixed time-length window, M, that shifts with every time step by *dt*. Values for M are in msec. The number of spikes is then divided by the maximum number of spikes for that window size (M), thus obtaining the firing rate. The maximum number of spikes for each window length was obtained from a 100 sec simulation of the network in the stable state. Finally, the firing rate is averaged for a fixed number (n) of the most recent windows. In this study, the detector parameters that are varied are the window size, M, and the number of windows that are averaged, n. These parameters take the following values: $M = \{25, 50, 100, 150, 200, 250\}$, $n = \{25, 50, 100, 150, 200, 250\}$.

The performance of the detector is thus analyzed in 72 scenarios; each scenario is a combination of a window size (M) with the number of windows averaged (n) and a unstable structural matrix that is used for the simulation of the unstable state ($\mathbf{W}_{u0}$ or $\mathbf{W}_{u200}$). The architecture of the detector that is proposed has two components: a cumulative likelihood generator and a threshold classifier described next.

1) Cumulative Likelihood Generator: From the measurements of p_k and the HMM emission distributions, the likelihood ratio is computed as follows: $LR_k \equiv q_2(p_k)/q_1(p_k)$.

When $LR_k > 1, p_k$ is more likely to belong to q_2 and hence the network is more likely to be unstable.

Once LR_k is computed, we then compute its cumulative;

$$gr_k = \sum_{n=1}^{k} LR(n)$$

The cumulative sum captures if p_k has been more likely to belong to q_2 ($LR_k >> 1$). If this is the case, gr_k will significantly increase. In order to determine if gr_k is showing a rapid increase, we take its derivative (dgr_k/dt), and detect if there is a sudden change indicating that p_k is generated from q_2.

2) Threshold Classifier: Detection occurs when the derivative of the cumulative likelihood ratio exceeds a threshold. Fig. 2 shows a successful instability detection and illustrates the behavior of the detector components. A threshold for each of the 72 scenarios is obtained from the mean average value of the (dgr_k/dt) over a 60 sec simulation of a unstable state network $\mathbf{W}_{u0}$ or $\mathbf{W}_{u200}$. The computed thresholds for each scenario are tested to find the combination of parameters for the detector that show a higher performance. Receiver Operating Characteristic (ROC) curves are obtained for each scenario. Each ROC curve captures the performance of 8 sub-thresholds that are obtained from each threshold. Sub-thresholds are a percentage of the computed threshold for a scenario, (e. g. 0.3, 0.4, 0.5, 0.6, 0.7, 0.8, 0.9, 1 of mean average of (dgr_k/dt) over a 60 sec simulation). In order to obtain the ROC curves we simulate the epileptic neuronal network for 10 sec where transition to unstable state might or not happen. For each sub-threshold 100 simulations were classified, in 50 of them transition to unstable state occurred. Sensitivity and fall-out were then computed for each parameter combination scenario for all simulations.

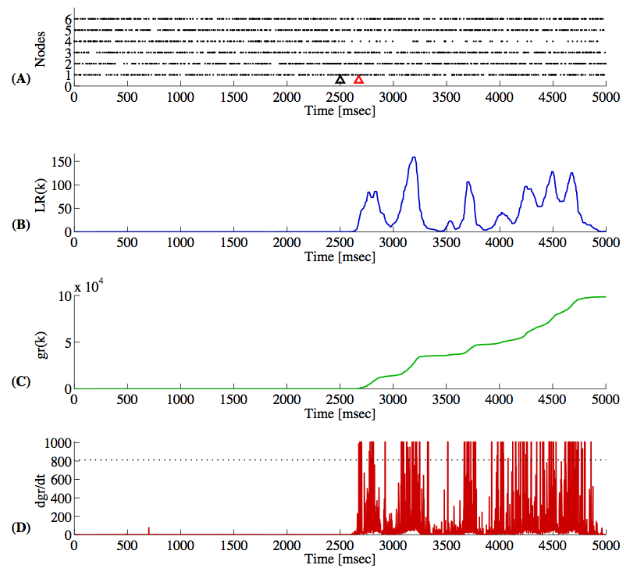

Fig. 2. Shows a 5 second simulation of the network. The network is initially stable and at t = 2.5 msec it is perturbed, taking λ_1 to 200 Hz. (A) Raster plots for all nodes in the network. The black arrow marks when the perturbation was done, the red arrow marks when it was detected. (B) Likelihood ratio of the observation distributions over time. (C) The cumulative function *gr* of the likelihood ratio over time. (D) The derivative of the cumulative function over time.

III. RESULTS

In this study, we assume that we have access to the spike trains of the network for both stable and unstable state. This is needed in order to compute the parameters of the HMM's emission distributions and the detector's threshold. In more realistic conditions, the degree of instability of the network that is being observed is unknown. Thus, we analyze the robustness of the detector's performance by analyzing the ROC curves results for the different unstable scenarios as if they were obtained from the same network. In order to analyze the results from the ROC curves, we collapsed the information from all the scenarios into 4 classes. These classes include in one scenario the ROC curve results for both unstable matrices, reducing the number of scenarios analyzed to 36.

0) : The scenario has $FPr > 0.05$ AND $TPr < 0.95$.
1) : The scenario has $FPr > 0.05$ AND $TPr > 0.95$.
2) : The scenario has $FPr < 0.05$ AND $TPr < 0.95$.
3) : The scenario has $FPr < 0.05$ AND $TPr > 0.95$.

Considering that a perfect classifier is defined as having $FPr = 0$ AND $TPr = 1$, a detector with parameters that fall into class 3 could be considered high performancing. Fig. 3 shows the results for the 36 different scenarios that were analyzed. In these scenarios, the detector parameters M and n are varied. From Fig. 3, it is clear that high performance was only obtained when using a window length of 250 msec.

For the detector proposed in this study, we encounter two types of delays; a detection delay, defined as the time between the actual transition to unstable and the detection time, and an initial delay due to window averaging when computing the firing rate of node 4. This is the time at the beginning of the simulation that the detector needs before being able to detect a transition. Both delays depend on the parameters M and n that are being used.

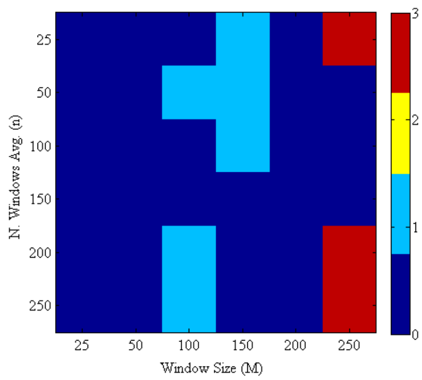

Fig. 3. Shows the class classification for each combination of the detector parameters, the colormap shows the color-class relation

In Table 1, detection and initial delays are shown for two class 1 detectors and for the three class 3 detectors. It is clear from these data that, M and n, independently affect both the detection and the initial delay. That is, when either M or n increase, the delays also increase. However, by comparing the delay values between detectors [100, 250] and [250, 25], we can conclude that the detection delay is mainly affected by M and the initial delay is mainly affected by n.

It is then reasonable to assume that if the window length were to be > 250 msec, the detection delay would be greater than the one found for class 3 detectors. This is not desirable since we aim to minimize the detection delay without compromising its performance, which is already achieved by the three class 3 detectors that were found. Therefore scenarios with bigger values of M were not considered. Results show that a detector with a window length of 250 msec that averages 25 windows has the best performance from the scenarios analyzed in this study. The optimal seizure-onset detector minimizes detection delay and maximizes the detection performance, in this study we derived a method to search for such high performance detector.

TABLE I
DETECTOR DELAYS

Detector $[M, n]$	**Detection Delay** [msec]	**Initial Delay** [msec]
[100, 50]	116 ± 37.5	157.6 ± 0.69
[100, 250]	281 ± 24.6	376.3 ± 1.73
[250, 25]	370 ± 100.2	279.9 ± 0.62
[250, 200]	468 ± 43.9	471.6 ± 1.77
[250, 250]	459 ± 29.5	526.3 ± 1.89

IV. CONCLUSIONS

The detector proposed in this study requires obtaining the firing rates in each state *a priori*. However, the detector showed high performance for seizure-onset detection of a stochastic neuronal network model. This study sets the stage for the design of a feedback control design that implements a high performance detector that then turns on or off a control input (e.g. electrical stimulation) to the most fragile node in the network to return it to its stable fixed point.

ACKNOWLEDGMENT

S. V. Sarma was supported by the Burroughs Wellcome Fund CASI Award 1007274. D. Ehrens was supported by the NIH Neuroengineering Training Program, 5T32EB00338310.

REFERENCES

[1] Ngugi A, Kariuki S, Bottomley C, Kleinschmidt I, Sander J and Newton C (2011) Incidency of epilepsy: a systematic review and meta-analysis. Neurology, 77(10), pp. 1005-12.

[2] Schuele S, Lüders H (2008) Intractable epilepsy: management and therapeutic alternatives. Lancet Neurology, 7, pp. 514-24.

[3] Santaniello S, SP Burns, J Madsen, J Singer, WS Anderson and SV Sarma (2011) Quickest Detection of Seizure Onsets in Drug-Resistant Patients: An Optimal Control Approach. Epilepsy & Behavior, Suppl1: S49-60.

[4] Uhlhaas PJ, Singer W (2003) Neural synchrony in brain disorders: Relevance for cognitive dys-functions and pathophysiology. Neuron 52: 599-625.

[5] Truccolo W, Donoghue JA, Hochberg LR, Eskandar EN, Madsen JR, et al. (2011) Single-neuron dynamics in human focal epilepsy. Nature Neuroscience 14: 635-643.

[6] DeFelipe J (1999) Chandelier cells and epilepsy. Brain 122: 1807-1822.

[7] Jin X, Prince DA, Huguenard JR (2006) Enhanced excitatory synaptic connectivity in layer v pyramidal neurons of chronically injured epileptogenic neocortex in rats. Journal of Neuroscience 26: 4891-4900.

[8] Bradford HF (1995) Glutamate, gaba and epilepsy. Progress in Neurobiology 47: 477-511.

[9] Traub RD, Whittington MA, Buhl EH, LeBeau FEN, Bibbig A, et al. (2001) A possible role for gap junctions in generation of very fast EEG oscillations preceding the onset of, and perhaps initiating, seizures. Epilepsia 42: 153-170.

[10] Sritharan D, Sarma SV. Fragility in Dynamic Networks: Application to Neural Networks in the Epileptic Cortex. Neural Computation (accepted for publication)

[11] Santaniello S, Sherman DL, Thakor NV, Eskandar EN, Sarma SV. Optimal Control-Based Bayesian Detection of Clinical and Behavioral State Transitions. IEEE Trans Neural Syt Rehabil Eng. vol. 4, pp. 708, September 2012

[12] Benayoun M, Cowan JD, van Drongelen W, Wallace E (2010) Avalanches in a stochastic model of spiking neurons. PLoS Computational Biology 6: 1-13.

[13] Gillespie DT (1977) Exact stochastic simulation of coupled chemical reactions. J Phys Chem 81: 2340-2361.